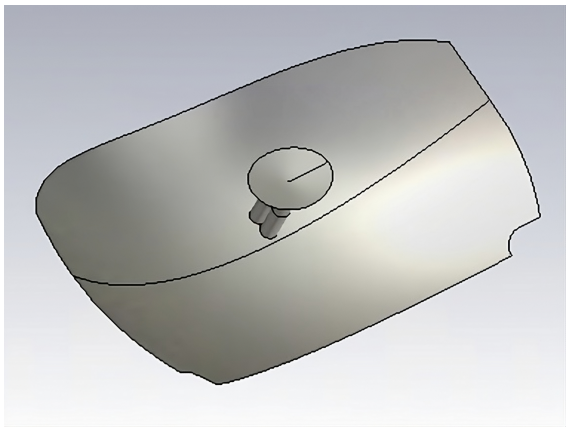

Aperture Efficiency of an Array Fed Truncated Cassegrain Reflector Antenna

A Comparison Between a Two Element Horn Array Feed and Single Horn Feed

Master's thesis in Wireless, Photonics and Space Engineering

VICTOR HENKOW

DEPARTMENT OF ELECTRICAL ENGINEERING

CHALMERS UNIVERSITY OF TECHNOLOGY
Gothenburg, Sweden 2024
www.chalmers.se

MASTER'S THESIS 2024

Aperture Efficiency of an Array Fed Truncated Cassegrain Reflector Antenna

A Comparison Between a Two Element Horn Array Feed and Single Horn Feed

VICTOR HENKOW

CHALMERS

Department of Electrical Engineering
CHALMERS UNIVERSITY OF TECHNOLOGY
Gothenburg, Sweden 2024

Aperture Efficiency of an Array Fed Truncated Cassegrain Reflector Antenna
A Comparison Between a Two Element Horn Array Feed and Single Horn Feed
VICTOR HENKOW

Supervisor: Thomas Schäfer, Satcube AB
Examiner: Jian Yang, Department of Electrical Engineering

Master's Thesis 2024
Department of Electrical Engineering
Chalmers University of Technology
SE-412 96 Gothenburg
Telephone +46 31 772 1000

Cover image: Model of a truncated Cassegrain truncated reflector antenna fed by a two element horn array.

Typeset in LaTeX
Gothenburg, Sweden 2024

Aperture Efficiency of an Array Fed Truncated Cassegrain Reflector Antenna
A Comparison Between a Two Element Horn Array Feed and Single Horn Feed
VICTOR HENKOW
Department of Electrical Engineering
Chalmers University of Technology

Abstract

If a reflector antenna needs to be mechanically steered, it can sometimes be necessary to truncate the sides of the main reflector to keep it from hitting the structure behind it. If the feed is kept circularly symmetric when the main reflector is truncated, it will lead to a low aperture efficiency. In this report a truncated Cassegrain reflector antenna was studied. The purpose was to investigate if the aperture efficiency could be improved by feeding the antenna with a two element horn array instead of a single horn. This was done by doing simulations in CST Studio Suite and optimizing using a Python script. Both types of feeds were modeled with the same limitations, so that the single horn antenna could act as a control. To improve the simulation time, the whole antenna was not optimized, instead the aperture efficiency was calculated from the feed using the spillover efficiency, the polarization efficiency, the illumination efficiency and the phase efficiency. The best single horn feed design had an aperture efficiency of $41\,\%$, and the best array feed design had an aperture efficiency of $49\,\%$. This indicates that the array feed is more efficient. However, the design that was tested was only a proof of concept, ignoring other efficiencies. The conclusion is that the concept shows potential, but more research needs be done before any conclusions about a realizable design can be made.

Keywords: truncated reflector, Cassegrain, dual reflector, array feed, aperture efficiency, asymmetrical reflector, elliptical beam, linear array feed, elliptical sub reflector.

Acknowledgments

This master's thesis has been conducted for the company Satcube AB. I must give a big thank you to the team at Satcube, who has welcomed me in to the company during the work of my thesis. My biggest thank you goes to my supervisor Thomas Schäfer. The completion of my thesis would not have been possible without his help.

Victor Henkow, Gothenburg, June 2024

Contents

1 Introduction **1**
1.1 Background . . . 1
1.2 Aim . . . 1

2 Theory **2**
2.1 General Antenna Theory . . . 2
2.1.1 Polarization . . . 2
2.1.2 Field Regions . . . 3
2.1.3 Power and Efficiency . . . 4
2.1.4 Noise . . . 5
2.2 Reflector Antennas . . . 6
2.2.1 Dual Reflector Antennas . . . 6
2.2.2 Aperture Efficiency . . . 8
2.2.3 Feed Antenna . . . 8

3 Method **10**
3.1 Implementations of Efficiency Equations in Python . . . 10
3.2 Test of Feed Efficiency Equations . . . 11
3.2.1 Custom Far Fields and Reflectors . . . 11
3.2.2 Comparison With Circularly Symmetric Equations . . . 12
3.3 Model and Simulation Set Up . . . 13
3.3.1 Designing the Model . . . 13
3.3.2 Choosing the Polarization . . . 14
3.3.3 Setting Up the Solver . . . 15
3.4 Optimization . . . 15

4 Result **16**
4.1 Feed Simulations . . . 16
4.2 Simulations Including the Main Reflector . . . 18

5 Discussion **19**
5.1 Interpretation of the Result . . . 19
5.1.1 Efficiency Equations . . . 19
5.1.2 Aperture Efficiency . . . 19
5.2 Future Research and Possible Improvements . . . 20
5.3 Writing Optimization Script . . . 20
5.4 Societal and Ethical Aspects . . . 20

6 Conclusion **21**

Appendices **24**
A LEO and GEO orbits . . . 24
B Parabolic Reflector in Spherical Coordinates . . . 24
C Circularly symmetric efficiency equations for parabolic reflector antennas . . . 25

1 Introduction

In this section a background to what will be investigated and why is presented. It also specifies the aim of the report.

1.1 Background

An internet connection normally requires substantial infrastructure on the ground. It is usually done via a direct connection with a fiber optic cable or wirelessly by connecting to a radio mast utilizing the cellular network. In some cases it is not reliable, or even possible to use ground based infrastructure. For example, in remote areas or in areas of conflict where it is at risk of being shut down. One solution is to connect to the internet using communication satellites instead. They can enable internet access for any area on Earth which are in the line of sight of them. Because of their high altitude compared with radio towers, they can cover much bigger areas making them ideal for remote locations. Since they are located in space and not in the same area as the user, they are also harder to tamper with for anyone controlling the area.

Communication satellites can be in different orbits. One type is geostationary orbits (GEO). Satellites in GEO are placed with an inclination and altitude so that they do not move relative to Earth's surface, making them appear stationary in the sky [1]. The benefit of this is that an antenna on Earth can be fixed in place, always pointing towards the same spot in the sky. One disadvantage with satellites in GEO is that they have to be at a high altitude, which means that the distance the signal has to travel is long. This creates problems with for example low received power and with high latency. Another type is low Earth orbits (LEO). LEO satellites are at relatively low altitudes. Because of this, they provide lower latency and higher receive power which enables higher data rates. Unlike GEO satellites, LEO satellites move relative to Earth's surface, which means that an antenna on Earth has to track the satellite's movement in the sky.

To get an antenna with high directivity, which is needed for high bandwidth satellite communication, it needs to have a large aperture. This can be achieved in many different ways. One way is with an array antenna. They use multiple antenna elements placed close enough together to interfere with each other, making them act like one single antenna. They can be designed with the ability to excite the elements with different phases, called a phased array. This allows them to steer their beam without moving the actual antenna. Array antennas are however complex and costly to manufacture, especially phased arrays. A more cost effective way to get a large aperture area is by using a reflector antenna. They use one or more reflectors to collimate the beam of a feed antenna to a plane wave. To steer the beam of a conventional reflector antenna, the whole antenna has to be mechanically rotated. A normal main reflector is circularly symmetric. In some cases, to get a large enough steering angle, the sides of the main reflector has to be truncated to keep it from hitting whatever is behind the antenna. Truncating the main reflector will lead to inefficiencies if the feed is not designed accordingly.

In this study, the antenna of a terminal made for satellite internet communication will be studied. The terminal is designed to work with both LEO satellites and with GEO satellites on moving vehicles. The terminal uses a truncated Cassegrain reflector antenna which is mechanically steered to track the satellites. A Cassegrain antenna is a type of dual reflector antenna. It has a parabolic main reflector and a convex hyperbolic sub reflector. Dual reflector antennas has the feed antenna pointing in the same direction as the main reflector. This is advantageous compared with a primary fed reflector when it comes to received noise and feed design.

1.2 Aim

The main goal of this study is to investigate if the aperture efficiency of a truncated Cassegrain reflector antenna can be improved by using a two element array feed antenna instead of a single element. The hypothesis is that this will give a field distribution which more effectively illuminates the main reflector. The reason is that the feed antenna will be more directive along the axis of

which the two elements are placed. The axis which have the highest directivity will then be placed along the narrowest axis of the main reflector, minimizing the spillover from the feed. Another aim is to derive equations for calculating the aperture efficiency from the far field of the sub reflector. To be able to calculate and compare different antenna configurations, models will be made, and simulations will be done in CST Studio Suite.

2 Theory

An antenna is a device that radiate or receive electromagnetic waves [2]. There are many types of antennas with different advantages for different applications and frequency ranges. There are some general concepts which are used to describe all antennas. There are also specific concepts for the antenna of interest. Both general and specific reflector antenna concepts are described in the sections below.

2.1 General Antenna Theory

To be able to describe, compare and choose an antenna design some general concepts needs to be understood.

2.1.1 Polarization

The propagating field of an antenna can always locally be considered a plane wave far enough away from the antenna [2]. A plane wave traveling in the $z-$direction can be written as

$$\boldsymbol{E}(z,t) = (\hat{x}Ae^{j\Phi_a} + \hat{y}Be^{j\Phi_b})e^{j\omega t - jkz}, \tag{1}$$

where A and B are real numbers, Φ_a and Φ_b are the phases of the field in the x and y direction respectively, ω is the angular frequency of the field, t is the time and k is the wave number, $k = 2\pi/\lambda$ where λ is the wavelength. The polarization of a plane wave is defined as the direction of the electric field over time [3]. In terms of (1) the polarization is given by the variation of the direction of

$$\vec{E}(z,t) = \Re(\boldsymbol{E}(z,t)) = \hat{x}E_x(z,t) + \hat{y}E_y(z,t), \tag{2}$$

where $E_x(z,t)$ and $E_y(z,t)$ is the electric field's x and y component. From (1) they can be derived to be

$$E_x(z,t) = A\cos(\omega t - kz + \Phi_a) \tag{3}$$
$$E_y(z,t) = B\cos(\omega t - kz + \Phi_b). \tag{4}$$

At a set distance z_0, the direction of (2) will generally trace an ellipse in the $x, y-$plane when time passes, shown in Figure 1a. The ratio between the two axis of the ellipse is determined by the relative sizes of A and B and their phase difference $\Phi = |\Phi_a - \Phi_b|$. If $\Phi = 0$ or π or if $A = 0$ or $B = 0$, one of the axis will be zero, which will trace a straight line, shown in Figure 1b. This is called linear polarization. If the line is aligned with the x-axis or the y-axis it is x-polarized or y-polarized respectively. If $A = B$ and $\Phi = \pi/2$, a circle will be traced as shown in Figure 1c. This is called circular polarization and can either be right-hand polarized or left-hand polarized, depending on which way the electric field rotates when time passes.

Instead of writing the polarization in terms of the spatial coordinates $\hat{x}$ and $\hat{y}$, it can be written in terms of a vector in the desired co polar direction $\hat{co}$ and the undesired cross polar direction $\hat{xp}$ [2]. The vectors are defined to be orthogonal unit vectors, i.e. they satisfy

$$\begin{aligned} |\hat{co}|^2 &= \hat{co}\cdot\hat{co}^*, \\ |\hat{xp}|^2 &= \hat{xp}\cdot\hat{xp}^*, \\ \hat{co}\cdot\hat{xp}^* &= 0, \\ \hat{xp}\cdot\hat{co}^* &= 0. \end{aligned} \tag{5}$$

Now (2) can be rewritten as

$$\vec{E}(z,t) = \hat{co}E_{co}(z,t) + \hat{xp}E_{xp}(z,t). \tag{6}$$

From (5) it is clear that there are two orthogonal polarizations. This can be utilized to send double the information over the same frequency band. For example, one message $a)$ can be sent over an x-polarized wave and one message $b)$ can be sent over a y-polarized wave. Then for $a)$ $\hat{x} = \hat{co}$ and $\hat{y} = \hat{xp}$, but for $b)$ $\hat{y} = \hat{co}$ and $\hat{xp} = \hat{x}$.

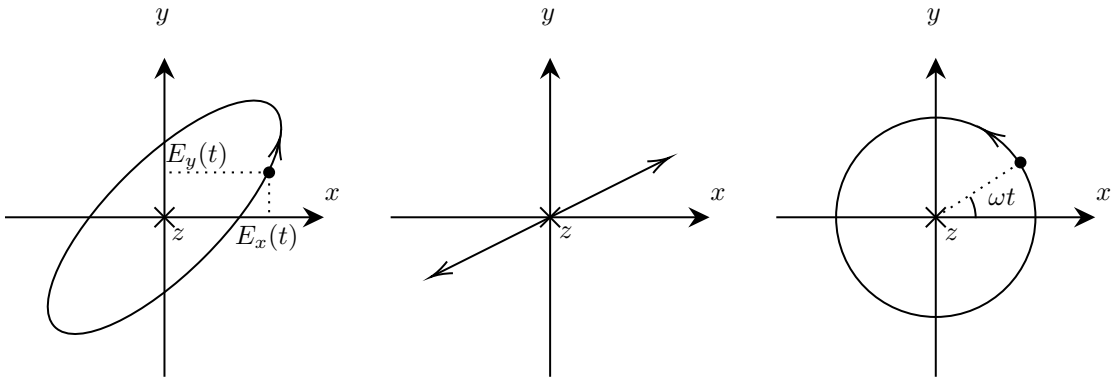

(a) General elliptical polarization **(b)** Linear polarization **(c)** Circular polarization

Figure 1: The $x, y-$plane at a fixed distance as time passes for an elliptically, linearly and circularly polarized wave.

2.1.2 Field Regions

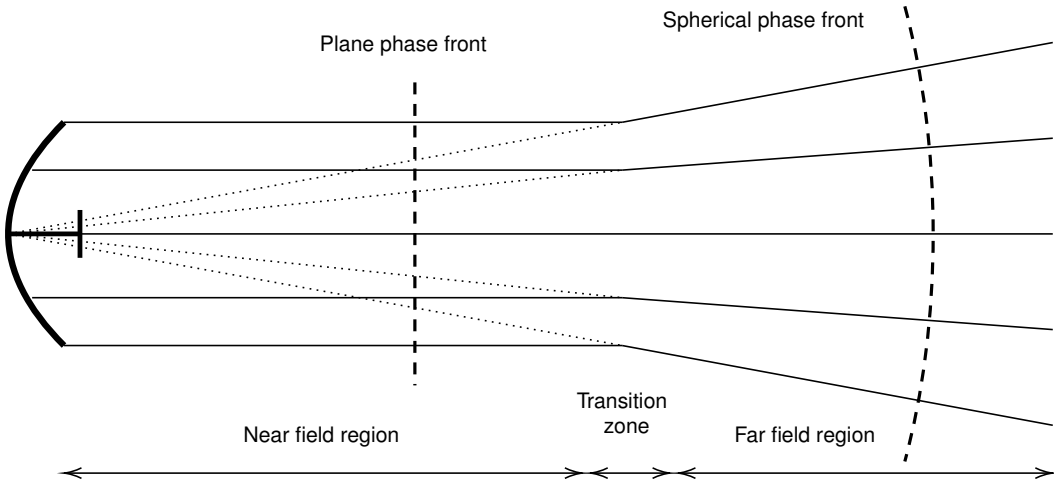

Figure 2: The figure shows the the idealized phase fronts for the near field region and the far field region.

The fields from an antenna can be split into two main regions, the near field and the far field, shown in Figure 2. In the near field region the electric field has a plane phase front [2]. Objects there are close enough to affect the transmitter. Antennas can be designed specifically for this region [4], but they are usually designed to work in the far field region. In the far field region, the phase front is spherical [2]. The far field region does not start at a specific point but instead gradually transitions. A rule of thumb for when it is safe to use the far field is [2]

$$r \geq \frac{2D^2}{\lambda}, \tag{7}$$

where D is the smallest diameter of a sphere containing all antenna components. Unlike objects in the near field, objects in the far field region do not affect the transmitter. When (7) is satisfied the electric field can be written as [2]

$$\boldsymbol{E}(r,\theta,\varphi) = \frac{1}{r}e^{j\omega t - jkr}\boldsymbol{G}(\theta,\varphi). \tag{8}$$

Here r is the distance from the antenna and $\boldsymbol{G}(\theta,\varphi)$ is called the far field function. This shows that it is possible to get the E-field for any large distance by just measuring the far field function at one distance. The far field function can be factorized in terms of its radiation pattern and phase function [2]. They have the following relation

$$\boldsymbol{G}(\theta,\varphi) = |\boldsymbol{G}(\theta,\varphi)|e^{j\Phi(\theta,\varphi)}, \tag{9}$$

where $|\boldsymbol{G}(\theta,\varphi)|$ is the radiation pattern and $\Phi(\theta,\varphi)$ is the phase function. Like the electric field, the far field function can also be split in to a co polar and cross polar component

$$\boldsymbol{G}(\theta,\varphi) = \hat{co}G_{co}(\theta,\varphi) + \hat{xp}G_{xp}(\theta,\varphi). \tag{10}$$

2.1.3 Power and Efficiency

The formulas below have been derived from [2]. To understand an antenna it is necessary to know how much power it is radiating. The time average Poynting vector is given by

$$\boldsymbol{S} = \frac{1}{2}\Re(\boldsymbol{E}\times\boldsymbol{H}^*). \tag{11}$$

It represents the time average power flow in a direction. For a plane wave, using (10), (8) and that $\boldsymbol{H} = \hat{z}/\eta \times \boldsymbol{E}$, it can be evaluated to be

$$\boldsymbol{S} = \frac{1}{2\eta r^2}|\boldsymbol{G}(\theta,\varphi)|^2 = \frac{1}{2\eta r^2}(|G_{co}(\theta,\varphi)|^2 + |G_{xp}(\theta,\varphi)|^2), \tag{12}$$

where η is the wave impedance. The total radiated power of an antenna is now calculated by integrating (12) over the whole far field sphere

$$P_{rad} = \int\int_S (\boldsymbol{S}\cdot\hat{r})dA = \frac{1}{2\eta}\int_0^{2\pi}\int_0^{\pi}(|G_{co}(\theta,\varphi)|^2 + |G_{xp}(\theta,\varphi)|^2)\sin(\theta)d\theta d\varphi. \tag{13}$$

An important measure of an antennas performance is the directive gain. It is the extra power transmitted by the co polar field in a given direction compared with an isotropic radiator with the same total radiated power,

$$D_g = \frac{|G_{co}(\theta,\varphi)|^2}{|G_{ISO}|^2}. \tag{14}$$

When characterizing an antenna, directivity is often used. It is the directive gain in the borsight direction,

$$D = \frac{|G_{co}(\theta,\varphi)|^2_{\max}}{|G_{ISO}|^2}. \tag{15}$$

The directivity can be calculated with

$$D = \frac{4\pi}{\lambda^2}Ae_{ap}, \tag{16}$$

where A is the aperture area of the antenna and e_{ap} is the aperture efficiency. By setting $e_{ap} = 1$, (16) gives the maximum directivity $D_{\max}$ a certain aperture can achieve. This gives the definition of aperture efficiency

$$e_{ap} = \frac{D}{D_{\max}}, \tag{17}$$

where D is the actual directivity. The antenna gain is a similar property to the directivity. The directivity compares the total radiated power for the co polar field with an isotropic antenna, the gain compares the power at the input of the antenna with an isotropic antenna. So it is defined as

$$G = e_{rad} e_{apol} D, \tag{18}$$

where e_{rad} is the radiation efficiency and e_{apol} is the alignment polarization efficiency. The alignment polarization efficiency is the cross polarization caused by non ideal antenna construction. The radiation efficiency is the ratio between the total radiated power from the antenna and the power delivered to the antenna input. The radiation efficiency can in turn be split in to two other efficiencies

$$e_{rad} = e_{abs} e_r, \tag{19}$$

where e_{abs} is the radiation efficiency due to absorption and $e_r = 1 - |\Gamma|^2$ is the radiation efficiency due to power reflecting back in to the antenna. The efficiency of an antenna is defined as the actual gain divided by the maximum possible gain

$$e_{ant} = \frac{G}{G_{\text{max}}}. \tag{20}$$

This gives a way to calculate the antenna efficiency by measuring the gain. Combined with the equations above it also implies that the antenna efficiency can be written in terms of the four subefficiencies

$$e_{ant} = e_{ap} e_{abs} e_r e_{apol}. \tag{21}$$

2.1.4 Noise

The maximum amount of information that can be sent over a channel is called the channel capacity C. It can be determined using the Shannon Hartley theorem [5]

$$C = B \log_2 \left(1 + \frac{P_{signal}}{P_{noise}} \right). \tag{22}$$

It shows that the channel capacity is bound by the the bandwidth B of the channel and the signal power P_{signal} in relation to the noise power P_{noise}. This means that it is not only important to design an antenna for high bandwidth and high gain to get a high receive power, it is also important to keep the signal to noise ratio (SNR) high by minimizing the received noise.

How much noise that is received depends on the antenna design, the environment which it is placed in and where it is looking. For example in a communication link between a satellite and a base station on the ground. The satellite will receive more noise because of thermal radiation from the relatively hot earth behind the base station, compared with the base station looking at the satellite with the cold space behind it.

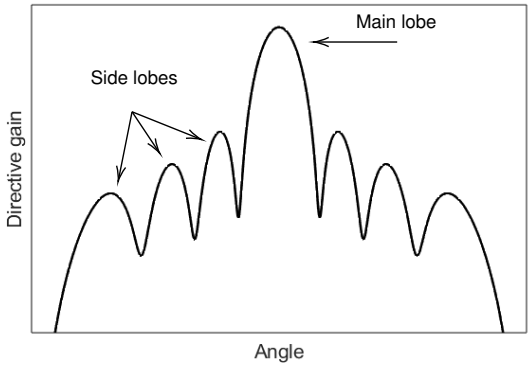

Figure 3: The main lobe is the biggest peak of the radiation pattern. The other peaks are the side lobes.

To keep noise down, the side lobe levels of both receiving and transmitting antennas should be considered when they are designed. Side lobes are all of the lobes which are not the main lobe of the antenna, as shown in Figure 3. The side lobe level is a measure of how big the side lobes are compared with the main lobe. For example, if an antenna has a directivity of $30\,$dBi and the first side lobe has a directive gain of $20\,$dBi, the side lobe level is $-10\,$dB.

For a transmitting antenna, large sidelobes lead to transmitting information in unintended directions, which can interfere with other communication links. For a receiving antenna, the antenna will receive extra power from the direction of the side lobes. If they are large it may significantly increase the received noise power because of both thermal radiation and interference.

2.2 Reflector Antennas

Reflector antennas use reflectors to collimate the beam of a feed antenna. They can come in different sizes, with different types of reflectors and with a different amount of reflectors.

2.2.1 Dual Reflector Antennas

A dual reflector antenna is an antenna with two reflectors. There are two main types, the Cassegrain reflector antenna and the Gregorian reflector antenna. The difference between them is whether the subreflector is concave or convex [6]. There are a few advantages to having a dual reflector antenna instead of a primary fed reflector antenna, which only has one reflector. The feed antenna is pointing in the same direction as the main reflector, this means that the spillover from the feed does not hit the warm ground which decreases the received noise power. Another reason is that the subreflector can be contoured to better illuminate the main reflector [7] which can increase efficiency. Since the feed antenna is pointing in the same direction as the main reflector, the feed is simpler to design.

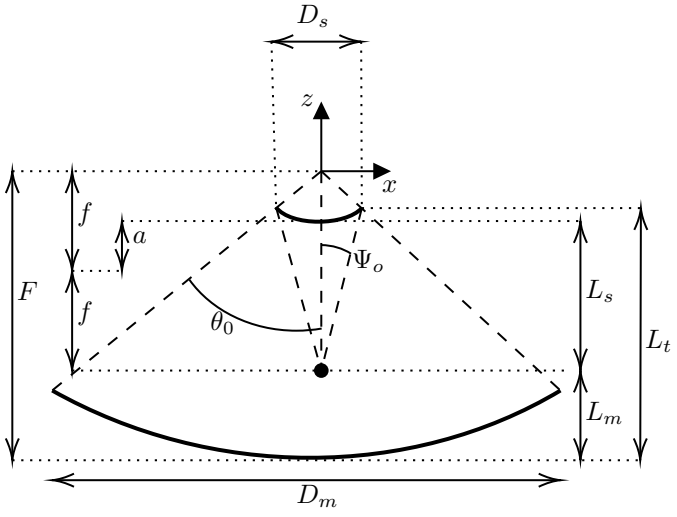

Figure 4: The geometry of a Cassegrain dual reflector antenna.

A Cassegrain antenna has a parabolic main reflector and a hyperbolic subreflector. The phase center of the feed antenna should be placed in the second focal point of the hyperbola, i.e if the focal point of the main reflector is at $(x, y) = (0, 0)$, it should be placed at $(x, y) = (0, -2f)$. The geometrical meaning of all important dual reflector parameters are shown in Figure 4. Its geometry can mathematically be described by four parameters. Four convenient ones are the main reflector diameter D_m, the subreflector diameter D_s, the main reflector's focal distance F and the opening angle of the feed antenna Ψ_0. It would be more useful to use the total length of the system L_t rather than F. However as seen in equation (33), L_t depends on F, a, D_s and f so

their expressions would get even more complicated if L_t was used instead of F. Since $L_T \leq F$, F can always be picked so that L_t does not exceed the maximum height of the system. L_T can also be calculated and then F can be adjusted to better fit the intended volume.

A Cassegrain antenna can be described using the equations introduced in this section [6]. The profile height of the main reflector with its focus in the origin is given by

$$\begin{gathered} z_{mr}(x_{mr}, y_{mr}) = \frac{x_{mr}^2 + y_{mr}^2}{4F} - F, \\ x_{mr}^2 + y_{mr}^2 \leq \frac{D_m^2}{4}. \end{gathered} \tag{23}$$

The profile height of the subreflector is then given by

$$\begin{gathered} z_{sr}(x_{sr}, y_{sr}) = a\sqrt{1 + \frac{x_{sr}^2 + y_{sr}^2}{f^2 - a^2}} - f, \\ x_{sr}^2 + y_s^2 \leq \frac{D_{sr}^2}{4}. \end{gathered} \tag{24}$$

The rest of the parameters will be written in terms of three helper equations Y_1, Y_2 and Y_3. They only serve to make the equations easier to read and is given by the following three equations

$$Y_1 = \tan\left(\frac{\Psi_0}{2}\right) F \tag{25}$$

$$Y_2 = 8FD_m - \sin(\Psi_0)(16F^2 + D_m^2) \tag{26}$$

$$\begin{aligned} Y_3 = -8D_m^2 F(D_s - 2\sin(\Psi_0)F) - 32\tan\left(\frac{\Psi_0}{2}\right) F^2 D_m(D_s + 2\sin(\Psi_0)F) + \\ + D_s \sin(\Psi_0)(16F^2 + D_m^2)(D_m + 4\tan\left(\frac{\Psi_0}{2}\right) F). \end{aligned} \tag{27}$$

The distance from the back of the main reflector to the phase center of the feed antenna is given by

$$L_m = \frac{Y_3}{16D_m \sin(\Psi_0)F(D_m + 4Y_1)}. \tag{28}$$

The distance from the feed's phase center to the back of the subreflector is given by

$$L_s = -\frac{D_s Y_2}{16\sin(\Psi_0)F(4Y_1) - D_m}. \tag{29}$$

A way to describe a hyperbola is by its eccentricity $e = c/a$. The parameters a and c also gives the focal length from

$$f = c - a, \tag{30}$$

where a is calculated with

$$a = \frac{D_s Y_2}{32\sin(\Psi_0)D_m F} \tag{31}$$

and c is

$$c = \frac{-D_s Y_2(D_m + 4Y_1)}{32\sin(\Psi_0)F(4Y_1)D_m - D_m}. \tag{32}$$

Now the total length of the entire antenna can be calculated with

$$L_t = F - c + a\sqrt{1 + \frac{D_s^2}{4(f^2 - a^2)}}. \tag{33}$$

2.2.2 Aperture Efficiency

An approximation of the aperture efficiency for a parabolic reflector antenna is the feed efficiency. It can be written as the product of four subefficiencies [8]

$$e_{ap} \approx e_{feed} = e_{sp} e_{pol} e_{ill} e_{\Phi}. \tag{34}$$

The subefficiencies are calculated from the far field that illuminates the main reflector. Which means for a dual reflector antenna, the subefficiencies are calculated from the field that has been reflected off the subreflector. For circularly symmetric antennas, equations for calculating them can be found in [8] and are presented in appendix C. Equations for non circularly symmetric antennas were derived from these equations and are presented below.

The first subefficiency is the spillover efficiency e_{sp}. It is the power within θ_0 divided by the total power radiated from the feed. For dual reflector antennas, spillover can occur either by missing the main reflector or by missing the subreflector. Like stated before, spillover from the main reflector will affect the received noise power more that spillover from the subreflector, this will however not make any difference on e_{sp}. The equation for calculating the spillover efficiency is

$$e_{sp} = \frac{\int_0^{2\pi} \int_0^{\theta_0(\varphi)} (|G_{co}(\theta,\varphi)|^2 + |G_{xp}(\theta,\varphi)|^2) \sin(\theta) d\theta d\varphi}{\int_0^{2\pi} \int_0^{\pi} (|G_{co}(\theta,\varphi)|^2 + |G_{xp}(\theta,\varphi)|^2) \sin(\theta) d\theta d\varphi}. \tag{35}$$

The power of the co polar field within θ_0 relative to the total power within θ_0 is given by e_{pol}. It is called the polarization efficiency. It represents the power lost in the cross polar field and is calculated with

$$e_{pol} = \frac{\int_0^{2\pi} \int_0^{\theta_0(\varphi)} |G_{co}(\theta,\varphi)|^2 \sin(\theta) d\theta d\varphi}{\int_0^{2\pi} \int_0^{\theta_0(\varphi)} (|G_{co}(\theta,\varphi)|^2 + |G_{xp}(\theta,\varphi)|^2) \sin(\theta) d\theta d\varphi}. \tag{36}$$

To utilize a reflector antennas aperture optimally, the reflectors surface needs to uniformly illuminated by the co polar field. This means that $|G_{co}(\theta,\varphi)| = 1/\cos^2(\theta/2)$ gives a perfect illumination of a parabolic reflector since $1/\cos^2(\theta/2)$ is a parabolic curve in spherical coordinates. A measure of how uniformly it is illuminated is the illumination efficiency e_{ill}. An expression for it is

$$e_{ill} = \frac{2 \int_0^{2\pi} \left(\int_0^{\theta_0(\varphi)} |G_{co}(\theta,\varphi)| \tan(\theta/2) d\theta \right)^2 d\varphi}{\int_0^{2\pi} \int_0^{\theta_0(\varphi)} \tan^2(\theta_0(\varphi)/2) |G_{co}(\theta,\varphi)|^2 \sin(\theta) d\theta d\varphi}. \tag{37}$$

The last subefficiency is the phase efficiency e_{Φ}. After the co polar field has been reflected off the main reflector the phase front should ideally be plane. Which means that a field illuminating the main reflector with a spherical phase front gives a perfect phase efficiency. The phase efficiency is a measure of this phase error and is calcualted with

$$e_{\Phi} = \frac{\int_0^{2\pi} \left| \int_0^{\theta_0(\varphi)} |G_{co}(\theta,\varphi)| e^{j\Phi_\delta} \tan(\theta/2) d\theta \right|^2 d\varphi}{\int_0^{2\pi} \left(\int_0^{\theta_0(\varphi)} |G_{co}(\theta,\varphi)| \tan(\theta/2) d\theta \right)^2 d\varphi}. \tag{38}$$

2.2.3 Feed Antenna

Many types of antennas can be used to feed a reflector antenna. One type that is well suited is the horn antenna. They are low loss, their directivity can be tuned and they are cheap and easy to manufacture [2]. They are made by cutting off a waveguide and to make them more directive the sides can be flared out, giving them a horn shape. Two of the most basic types of horn antennas are the pyramidal horn and the conical horn, which are shown in Figure 5.

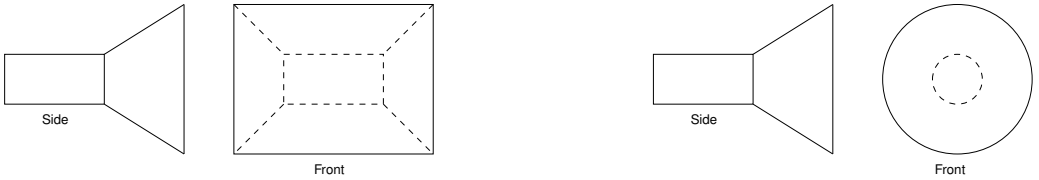

(a) Pyramidal horn **(b)** Conical horn

Figure 5: Two different kinds of horn antennas.

Feed antennas does not have to be a single antenna element, it can also be an array of multiple antenna elements. It could for example be four horns placed close together. Array antennas can have many benefits. For example, they can be used to get a more directive beam on one axis by placing more elements on that axis. Different elements can be used for receiving and for transmitting, which can help with isolation between polarizations, or if transmission and receiving is done on different frequency bands, different antenna elements could be designed for the different bands. Array antennas have some disadvantages compared with single antennas though. Firstly, they are more complex to realize. They will also get grating lobes if the antenna elements are spaced too far apart. A grating lobe is an undesired lobe that comes from the phase difference between the antenna elements [2]. For a two element array the distance between the elements should be less than 0.5λ to avoid getting grating lobes [2]. Figure 6 shows plots of the phase fronts and the radiation pattern for a two element array, both when the elements are placed close together and too far apart.

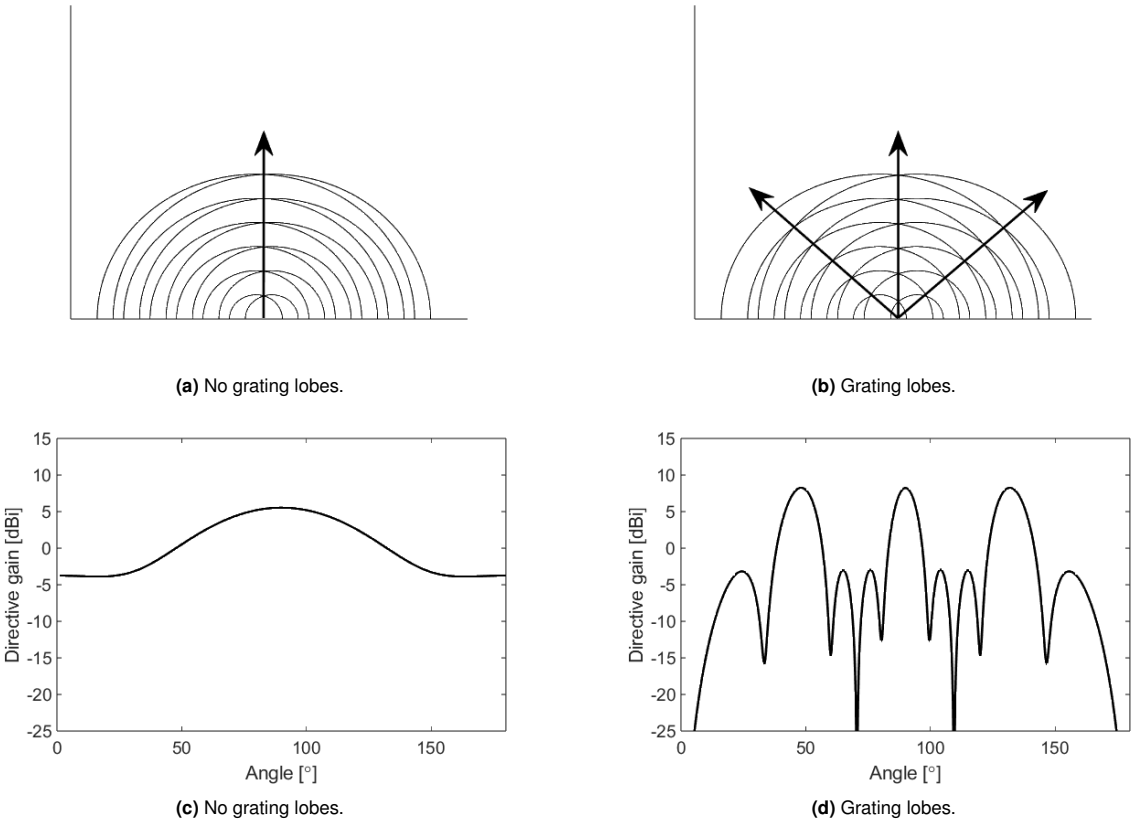

(a) No grating lobes. **(b)** Grating lobes.

(c) No grating lobes. **(d)** Grating lobes.

Figure 6: The plots are showing a two element antenna array both when the elements are placed close together and far apart. Figure 6a and 6b shows the phase fronts of the antenna array. The arrow indicates where the waves interfere fully constructively. Figure 6c and 6d shows shows their radiation patterns.

3 Method

In this study a Cassegrain antenna with a truncated main reflector was investigated. A summary of the design limitations are presented in Table 1. The feed antenna was an array of two conical horns and the goal was to see if it would provide a higher aperture efficiency than a single horn feed antenna. To be able to do this comparison both variants of the antenna was designed and simulated in the electromagnetic simulation program CST Studio Suite [9]. The program was controlled by Python [10] [11] which used the Nelder-Mead minimization algorithm [12] [13] to tune parameters until the optimum aperture efficiency was achieved. More detailed descriptions of the method is presented in the sections below.

Table 1: Summary of design limitations.

Center frequency	$19.5\,\text{GHz}$
Polarization	Linear
Antenna type	Cassegrain dual reflector
Main reflector	Provided by Satcube, see Figure 10d
Feed antenna	Array of two horn antennas
Waveguide type	Circular
Simulation software	CST studio suite

3.1 Implementations of Efficiency Equations in Python

Python was used to calculate the aperture efficiency. Firstly, the data about $|G_{xp}(\theta,\varphi)|$, $\Phi_{xp}(\theta,\varphi)$, $|G_{co}(\theta,\varphi)|$ and $\Phi_{co}(\theta,\varphi)$ for $0^\circ \leq \theta \leq 180^\circ$ and $0^\circ \leq \varphi \leq 360^\circ$ were imported to Python. Then, the field inside the main reflector was selected. The selection of the data was done by first importing the coordinates of the main reflector's geometry. Then the outline of the main reflector $\theta_{outline}(\varphi)$ was determined by finding $\max(\theta)$ for every φ. It is shown as the black dashed line in Figure 7. The data points closest to the outline of the main reflector was set to the opening angle $\theta_0(\varphi)$. So it was found by calculating $\theta_0(\varphi) = \min(|\theta_{outline}(\varphi) - \theta_{data}(\varphi)|)$. The data for the points where $\theta > \theta_0(\varphi)$ was set to the same values as the points where $\theta = \theta_0(\varphi)$. This gives the same effect as removing the data outside of $\theta_0(\varphi)$, and removing the data was not possible since every row in a matrix needs to have the same amount of columns. An example of how the data gets selected is shown in Figure 7. The data points are shown in gray. The first picture shows the initial data and the second one shows how all of the data points outside of the main reflector has been discarded.

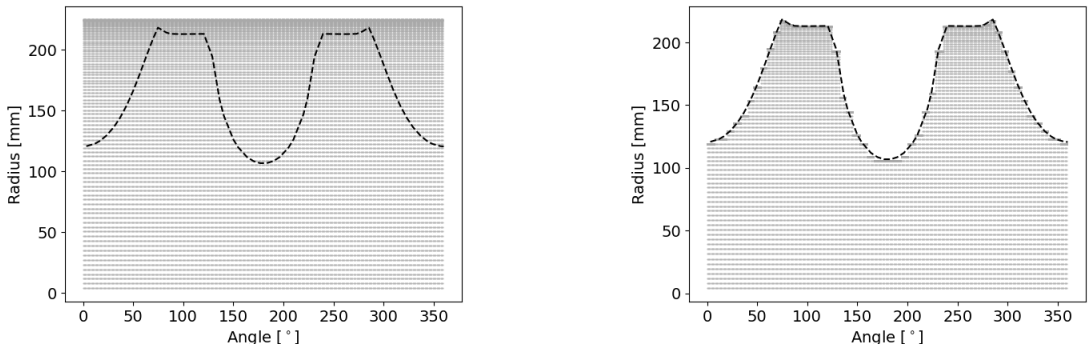

Figure 7: The plots show the far fields data points in gray and the outline of the main reflector is the dashed black line. It shows for which points there is data initially, and after the data outside the main reflector has been removed.

To calculate the aperture efficiency, (17) together with (35) - (38) was used. The integrals in the equations were implemented using numpy.trapz [14], which calculates integrals using the

trapezoidal rule. This is why a way of discarding the data outside of the main reflector was needed. The integration function integrates over all the data which it is given, which means that the integration bounds are set by the data points.

3.2 Test of Feed Efficiency Equations

Since (37) - (38) was derived for this study, they needed to be tested to verify that they give answers that are as expected. It was done by first using custom created fields and reflectors, and then by comparison to already established equations valid for circularly symmetric antennas.

3.2.1 Custom Far Fields and Reflectors

The two custom far fields used are shown in Figure 8, and the three reflectors are shown in Figure 9. These reflectors and fields were used together to create combinations which had known efficiencies for the different equations. The expected value was then compared with the calculated one to verify that they gave the same result.

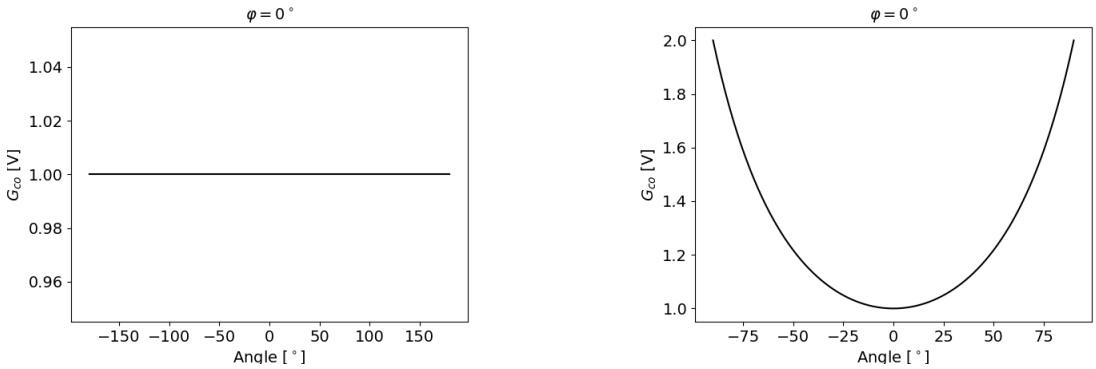

Figure 8: Plots of the far fields used to verify the efficiency equations. Figure 8a shows $|G_{co}(\theta, \varphi)| = 1$ and 8b shows $|G_{co}(\theta, \varphi)| = 1/\cos^2(\theta)$.

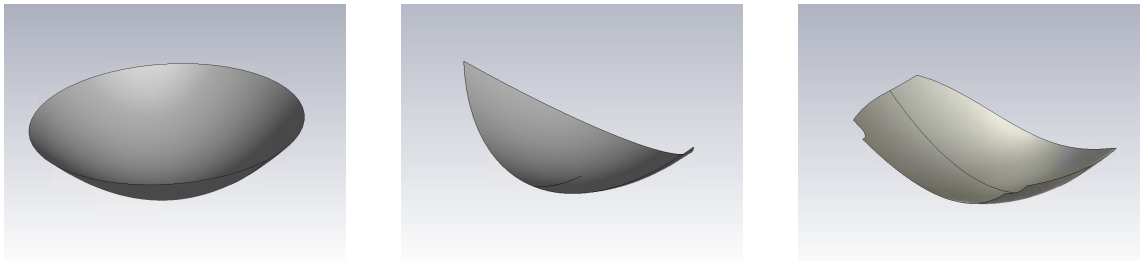

Figure 9: Models of the reflectors used to verify the efficiency equations. Figure 9a shows a parabolic reflector with $\theta_0 = 90°$, 9b shows a reflector made from a quarter of a sphere and 9c shown the parabolic reflector used in the real design.

All of the test cases are shown in Table 2. The first efficiency that was tested was the spillover efficiency. It was tested using an isotropic co polar radiation pattern shown in Figure 8a and the two reflectors shown in Figure 9a and Figure 9b. Since they are used together with an isotropic radiator, $50\,\%$ and $25\,\%$ of the field should hit them. Which also is what the efficiency calculation gives.

The second efficiency that was tested was the polarization efficiency. If all of the radiated power within $\theta_0(\varphi)$ is in the co polar field, it should give $e_{pol} = 1$. If an equal amount of power is in the cross polar field, it should give $e_{pol} = 0.5$. This should be true no matter how the main reflector looks. This is why the polarization efficiency was tested using both patterns in Figure 8 and two different reflectors. The calculated answers were the same as the expected answers.

The illumination efficiency was tested using the parabolic co polar radiation pattern shown in Figure 8b. It should give a perfect illumination of any parabolic reflector. It was tested using the two parabolic reflectors in Figure 9. The calculated values matched the expected answers.

The last equation to test was the phase efficiency. The phase efficiency should be perfect for any parabolic reflector and any radiation pattern, as long as the far field function has a spherical phase front. It was tested using both parabolic reflectors in Figure 9 and both co polar radiation patterns in Figure 8. The phase function was set to $\Phi(\theta, \varphi) = 180°$, giving it a spherical phase front. The equations gave expected answers.

Table 2: Different test cases used to verify the efficiency equations.

Field	Reflector	Expected	Calculated
$\boldsymbol{e_{sp}}$			
$\lvert G_{co}(\theta,\varphi)\rvert = 1$	9a	0.5	0.493
$\lvert G_{co}(\theta,\varphi)\rvert = 1$	9b	0.25	0.251
$\boldsymbol{e_{pol}}$			
$\lvert G_{co}(\theta,\varphi)\rvert = 1$, $G_{xp}(\theta,\varphi) = 0$	9a	1	1.00
$\lvert G_{co}(\theta,\varphi)\rvert = 1$, $G_{xp}(\theta,\varphi) = 1$	9a	0.5	0.500
$\lvert G_{co}(\theta,\varphi)\rvert = 1$, $G_{xp}(\theta,\varphi) = 0$	9b	1	1.00
$\lvert G_{co}(\theta,\varphi)\rvert = 1$, $G_{xp}(\theta,\varphi) = 1$	9b	0.5	0.500
$\lvert G_{co}(\theta,\varphi)\rvert = 1/\cos^2(\theta)$, $\lvert G_{xp}(\theta,\varphi)\rvert = 1/\cos^2(\theta)$	9a	0.5	0.500
$\boldsymbol{e_{ill}}$			
$\lvert G_{co}(\theta,\varphi)\rvert = 1/cos^2(\theta)$	9a	1	1.00
$\lvert G_{co}(\theta,\varphi)\rvert = 1/cos^2(\theta)$	9c	1	1.00
$\boldsymbol{e_{\Phi}}$			
$\Phi_{co}(\theta,\varphi) = 180$, $\lvert G_{co}(\theta,\varphi)\rvert = 1/cos^2(\theta)$	9c	1	1.00
$\Phi_{co}(\theta,\varphi) = 180$, $\lvert G_{co}(\theta,\varphi)\rvert = 1/cos^2(\theta)$	9a	1	1.00
$\Phi_{co}(\theta,\varphi) = 180$, $\lvert G_{co}(\theta,\varphi)\rvert = 1$	9c	1	1.00

3.2.2 Comparison With Circularly Symmetric Equations

The equations were also compared with the ones valid for circularly symmetric antennas found in Appendix C. For a circularly symmetric antenna, both types of equations should give the same answer. Table 3 shows the answers of the equations when an open ended circular waveguide was used as the antenna. The equations agree well with each other. This test together with the ones done in Table 2 indicate that the new equations are correct.

Table 3: Comparison between calculated efficiencies for a circular waveguide using circularly symmetric and general parabolic efficiency equations.

Efficiency	Circularly symmetric	General
e_{sp}	0.934	0.934
e_{pol}	0.997	0.998
e_{ill}	0.633	0.635
e_{Φ}	0.996	0.986

3.3 Model and Simulation Set Up

CST studio suite was used to design and simulate the antennas. Two types were designed, one with a two element array horn feed and a reference design with a single conical horn.

3.3.1 Designing the Model

A model with a two element array feed and a model with single element feed was created. Both feeds would have the same initial dimensions and they would be optimized using the same parameters. This would make sure that there was two comparable feeds. The models would act as the base of the optimization.

The first step to building the models was to input (25) - (22) to the parameter list in CST. The initial values used for the design are shown in Table 4. It also shows which of these values comes from the design of the main reflector, which are set to fixed values and which are going to be used in the optimization. The table has a description of the parameters, but Figure 10 also shows the parameters geometrically. It also shows how the coordinate system is defined.

Table 4: Values that were used to make the initial model of the sub reflector and feed. D_m is the value along the non truncated axis and D_s along the longest axis of the ellipse. L_a does not apply to the single feed.

Determined by the main reflector		
Parameter	**Value**	**Description**
D_m	$450\,\text{mm}$	Main reflector diameter
F	$112.5\,\text{mm}$	Main reflector focal distance
Set values		
Parameter	**Value**	**Description**
L_{wg}	$30\,\text{mm}$	Length of the waveguides
D_{wg}	$11.56\,\text{mm}$	Inner diameter of the waveguides
T	$1.0\,\text{mm}$	Thickness of the waveguides' walls
Initial values to be optimized		
Parameter	**Value**	**Description**
D_s	$70\,\text{mm}$	Sub reflector diameter
Ψ_0	62°	Opening angle of feed antenna
R	0.70	Ratio between elliptical subreflector axis
L_h	$20\,\text{mm}$	Length of the feed antenna horn taper
D_h	$0\,\text{mm}$	Diameter of the feed antenna horn
H_o	$0\,\text{mm}$	Horizontal offset of the horn antenna
L_a	$0\,\text{mm}$	Distance between feed array horn walls

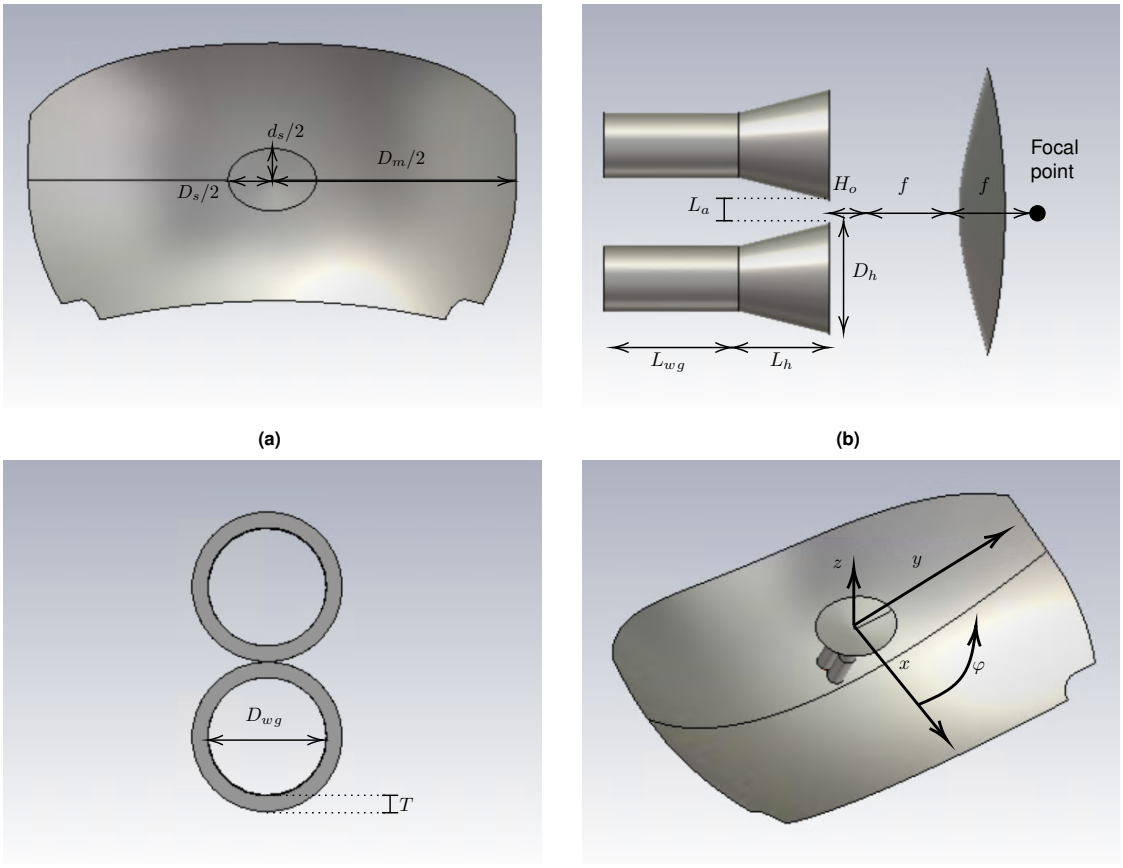

Figure 10: The CST model of the Cassegrain antenna is shown in the pictures. Note that $R = d_s/D_s$.

The feed antenna consisted of one or two circular waveguides, for the reference design and the concept respectively, where the end could be flared out to a conical horn. The waveguide was made for 19.5 Ghz, which gave it $D_{wg} = 11.52$ mm according to the standard waveguide sizes in [15]. The axis with only one horn for the array feed with $D_h = 0$ had a 3 dB beam width of $62°$ so this was chosen as the opening angle of the feed antenna. R was chosen to 0.7 because it matched the shape of the main reflector well.

Once the values were in the parameter list in CST, the subreflector could be made. The profile height of the sub reflector was made using (24) with $y_{sr} = 0$ and $0 \leq x_{sr} \leq D_s/2$. This gave a hyperbolic curve along the x-axis from 0 to $D_{sr}/2$. The hyperbolic curve was then rotated around the z-axis to give a circularly symmetric sub reflector. This sub reflector was then truncated by an ellipse with a semi major axis $D_s/2$ and a semi minor axis $d_s/2$, which were given by the ratio $R = d_s/D_s$.

3.3.2 Choosing the Polarization

The polarization was limited to linear, but if x- or y-polarization was going to be used needed to be decided. This was tested by setting up both polarizations for the dual waveguide feed antenna, and studying the radiation patterns. Figure 11 shows how the fields look for the cross sections $\varphi = 0°$ and $\varphi = 90°$. The patters are very similar, but since the y-polarization has a smaller back lobe, it was picked.

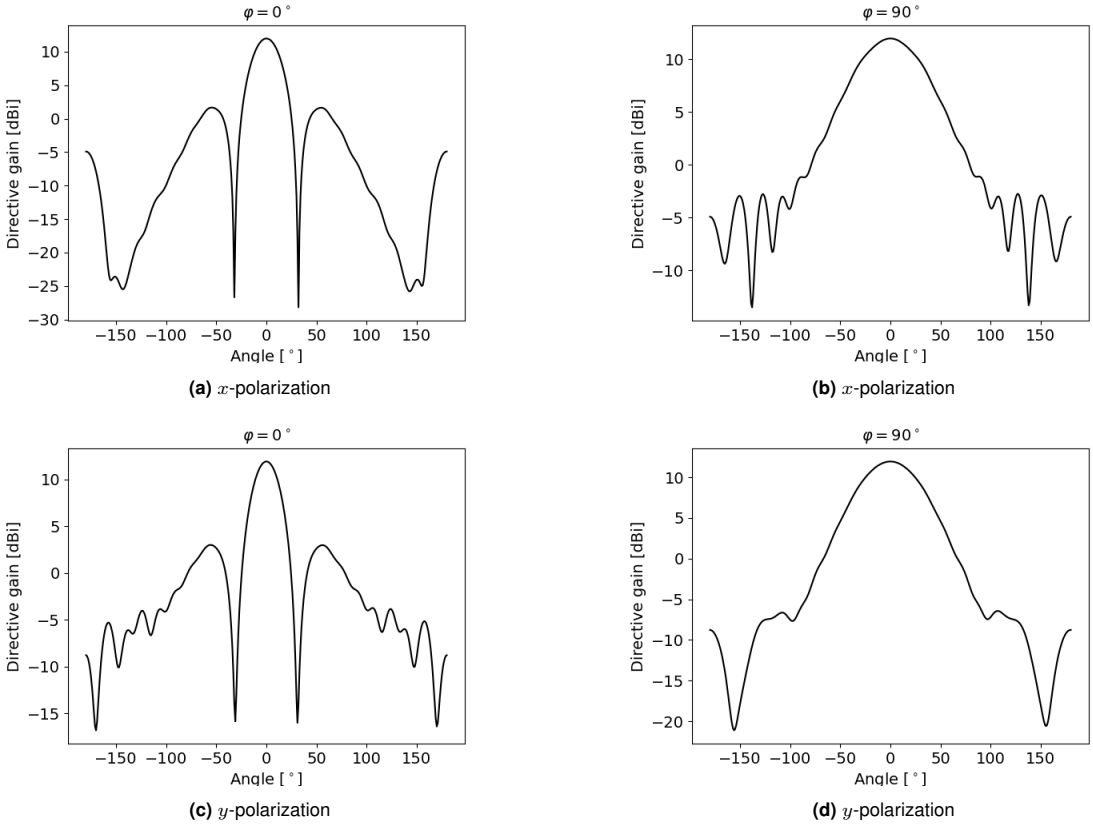

(a) x-polarization **(b)** x-polarization

(c) y-polarization **(d)** y-polarization

Figure 11: Directive gain for a two horn array when $L_a = 0$ when the field is x-polarized and y-polarized. The figures shows two cuts along $\varphi = 0°$ and $\varphi = 90°$ where φ is defined as the angle from the x-axis.

3.3.3 Setting Up the Solver

CST has multiple solvers [16] which are used for simulating electromagnetic devices. For this study the Frequency Domain Solver was used. It is a general high frequency solver for small to medium sized devices. It was set up for the frequency span $18 - 21$ GHz with a far field monitor at 19.5 GHz. Two symmetry planes were used to improve the simulation time, a magnetic symmetry in the y, z-plane and an electric symmetry in the x, z-plane. A result template was set up to export the far field to a file every time the solver was run, which was used to import the field data to Python. The file gave the data points of the far field for every $1°$ in both the θ- and φ-direction.

3.4 Optimization

The optimization of the aperture efficiency was done in the same way for both feed designs. It was done without the main reflector. Instead of calculating the aperture efficiency from the far field of the entire antenna, it was done using the far field of the feed antenna and the sub reflector with (17). The reason for this is that it significantly improves the simulation time which in turn makes the optimization feasible. The built in optimizer in CST can not work towards any goal. Since (35), (36), (37) and (38) could not be entered in to CST, an optimization script had to be set up with Python. The code can be downloaded from [17].

The optimization was based on the Nelder-Mead minimization algorithm from SciPy [12]. It started with the parameter values given in Table 4. It then ran the simulation in CST. When the simulation was done, the values were imported to Python and the aperture efficiency was calculated. Since the aperture efficiency should be maximized, $1 - e_{ap}$ was returned to the Nelder-Mead min-

imization function. It then tweaked the parameters given in Table 5. The parameters were not allowed to have any value, they were only allowed to be changed within some bounds that were considered reasonable. Once the Nelder-Mead algorithm had fullfilled its minimization critera with a tolerance of 0.01, it returned the parameters which gave the highest aperture efficiency.

Table 5: Parameters that were used to optimize the designs. L_a is only used for the two horn array feed.

Parameter	Bounds
D_s	$[30, 85]$ mm
Ψ_0	$[22.5°, 85°]$
R	$[0.4, 1]$
L_h	$[10, 70]$ mm
D_h	$[0, 30]$ mm
H_o	$[-40, 30]$ mm
L_a	$[0, 20]$ mm

The aperture efficiency was also verified by simulating the feed which gave the best aperture efficiency with the main reflector. This gave the directivity of the entire antenna. Because of the main reflector's shape, only one symmetry plane could be used. A magnetic symmetry in the y, z-plane. The maximum directivity of the Cassegrain antenna is given by (16) as

$$D_{\max} = \frac{4\pi(19.5 \cdot 10^9)^2}{(3 \cdot 10^8)^2} \cdot 0.0897 = 36.78\,\text{dBi}.$$

Now (17) was used to find the aperture efficiency. To make sure that the feed was located in the optimum position relative to the main reflector, a parametric sweep was done to test different positions of the main reflector. First 5 points were tested from -3 mm to $+3$ mm relative to the original position of the main reflector. Then another sweep was done for three positions around the position with the highest directivity.

4 Result

The parameters and efficiencies obtained from the optimizations of the single feed antenna and the two element array feed antenna are presented below. The directivity and aperture efficiency of simulations including the main reflector are also presented.

4.1 Feed Simulations

The design parameters for both the two element horn array feed and the single element horn feed which the optimizer found to give the best aperture efficiency are displayed in Table 6. The corresponding aperture efficiencies and its sub efficiencies are shown in Table 7. It shows that the spillover efficiency was 0.17 higher for the array feed than the single feed and that the aperture efficiency was 0.08 higher. The other efficiencies were higher for the single feed. The polarization efficiency was 0.01 higher, the illumination efficiency was 0.04 higher and the phase efficiency was 0.02 higher.

Table 6: Optimized parameter values.

Parameter	Array Feed	Single Feed
D_s	$81.29\,\text{mm}$	$73.58\,\text{mm}$
Ψ_0	$70.07°$	$68.75°$
R	0.7191	1.000
L_h	$20.00\,\text{mm}$	$22.10\,\text{mm}$
D_h	$0\,\text{mm}$	$1.530\,\text{mm}$
H_o	$1.563\,\text{mm}$	$0\,\text{mm}$
L_a	$0\,\text{mm}$	-

Table 7: The calculated efficiencies for the optimized feeds.

Efficiency	Array Feed	Single Feed
e_{sp}	0.61	0.44
e_{pol}	0.95	0.96
e_{ill}	0.93	0.97
e_{Φ}	0.90	0.92
e_{ap}	0.49	0.41

Plots of the radiation patterns which were used to calculate the efficiencies above are shown in Figure 12 and 13. Figure 12 shows the patterns across the cross sections $\varphi = 0°$ and $\varphi = 90°$. Figure 13 shows the patterns in 3D.

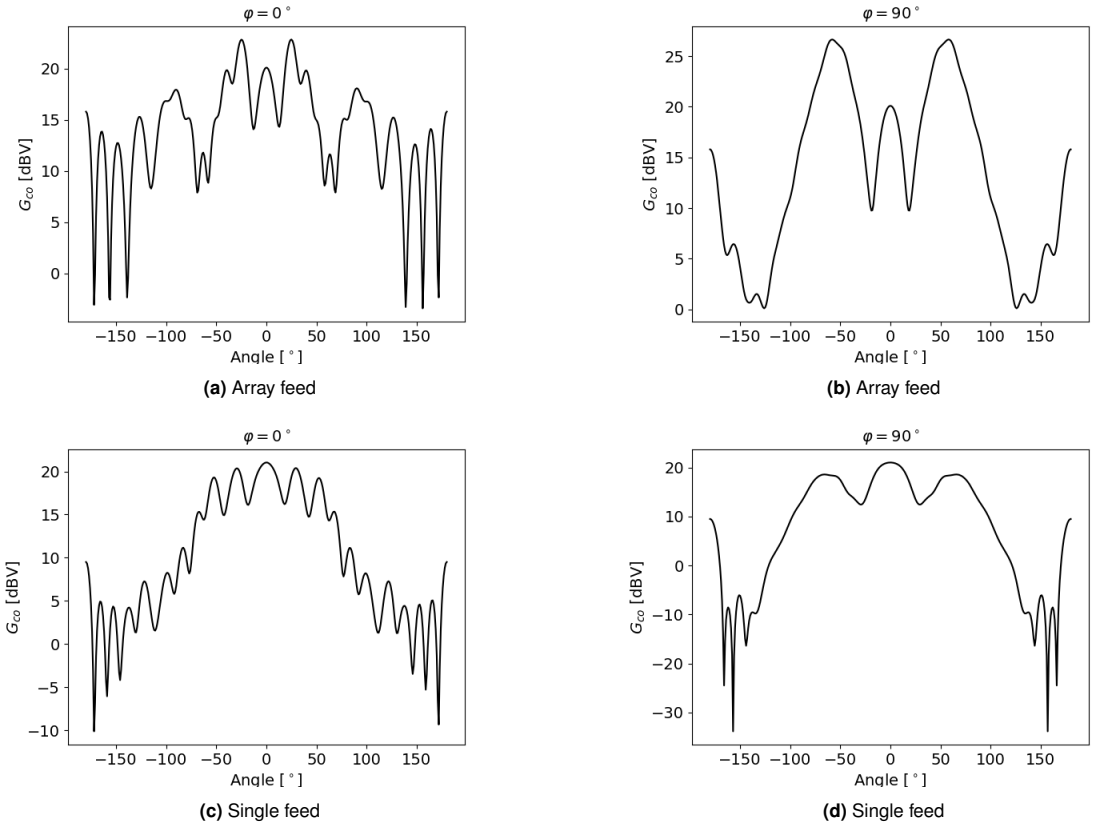

(a) Array feed

(b) Array feed

(c) Single feed

(d) Single feed

Figure 12: $|G_{co}(\theta, \varphi)|$ for different cross sections.

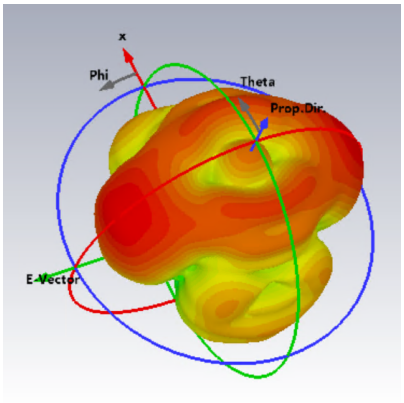

(a) Array feed

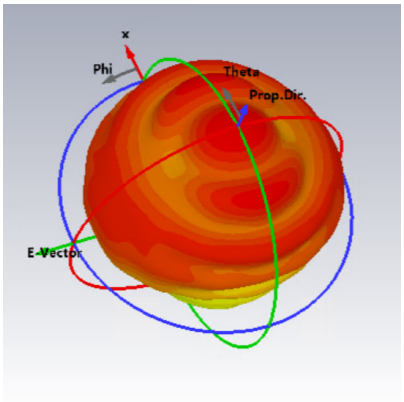

(b) Single feed

Figure 13: $|G_{co}(\theta, \varphi)|$ for both feeds in 3D.

4.2 Simulations Including the Main Reflector

Figure 14 shows the directive gain for the entire antenna with both feeds for the cross sections $\varphi = 0°$ and $\varphi = 90°$. The directivity of the antenna with the array feed is 33.2 dBi which gives an aperture efficiency of 0.44. When $\varphi = 0°$ the sidelobe level is -15.5 dB and when $\varphi = 90°$ it is -12.8 dB. The directivity of the antenna with the single feed horn is 32.7 dBi which gives an aperture efficiency of 0.39. It has a sidelobe level of -14.8 dB when $\varphi = 0°$ and -13.2 dB when $\varphi = 90°$.

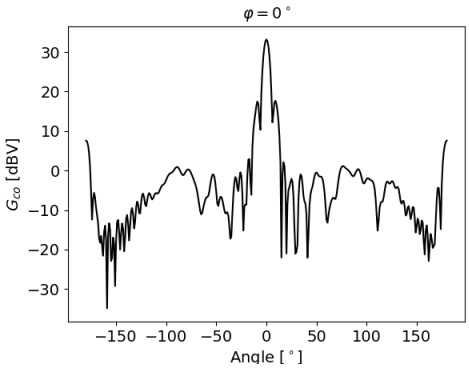

(a) Array feed

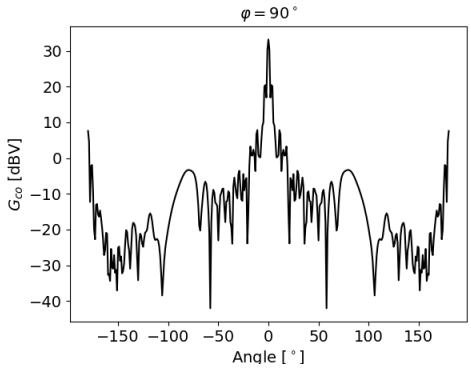

(b) Array feed

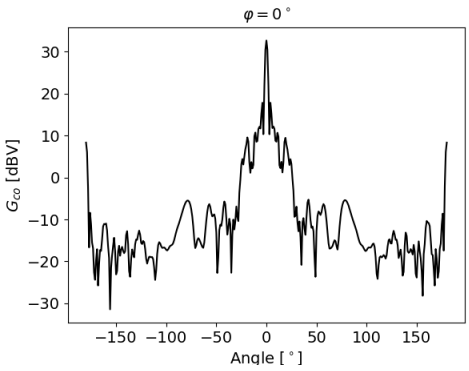

(c) Single feed

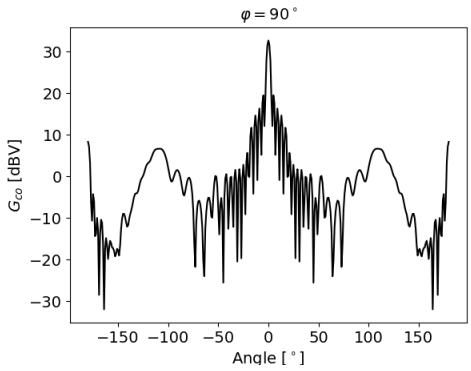

(d) Single feed

Figure 14: Directive gain for different cross sections.

5 Discussion

Different aspects of the method and result are discussed in the sections below.

5.1 Interpretation of the Result

This study aimed to find equations which could calculate the aperture efficiency of a non symmetric parabolic reflector antenna from the far field of the sub reflector. It also aimed to investigate if the aperture efficiency of a reflector antenna with a truncated main reflector could be improved by using an array feed. The results are discussed according to these aims. The method used is also discussed and where discrepancies may have come from.

5.1.1 Efficiency Equations

Equations for calculating the aperture efficiency of an asymmetrical parabolic reflector antenna were derived, seen in (35) - (38). They were first verified to agree with the expected values for some special cases. When they were used on a circularly symmetric antenna, they were also shown to give the same answer as the already established equations.

The optimization was done using (35) - (38) from the far field of the subreflector. Once the optimum parameters were found, a simulation pass was also done including the main reflector for both the two element array feed and the single element feed. This showed a difference 0.05 for the array feed and 0.02 for the single feed. The difference is probably due to two factors. Firstly, (17) is only an approximation. Two other factors which could be added to make it more accurate are a diffraction efficiency and a blockage efficiency [2]. Secondly, the equations assume that the feed is placed at the optimum position. To find this position, a parametric sweep moving the main reflector was done. However, since the simulation time was ~ 8 h, only eighth different positions were tried. This means that it was probably possible to find a better position for the main reflector relative to the feed, which would increase the directivity.

5.1.2 Aperture Efficiency

For the models designed in this study, the aperture efficiency was 0.08 higher for the two element array feed compared with the single element feed when it was calculated from the sub reflectors. When it was calculated from the main reflector it was 0.05 higher. This indicates that the aperture efficiency of a truncated Cassegrain reflector antenna can be increased by having a two element array feed antenna. Furthermore, the increased aperture efficiency is only due a higher spillover efficiency. All of the other sub efficiencies were lower for the array feed. Little spillover is extra important when it comes to receiving antennas since it decreases noise which allows the antenna to distinguish a message with a lower receive power.

The optimization was done using the Nelder-Mead algorithm. This is a local optimizer which means that the initial parameters are important. To make the two feeds comparable, the same initial values were used. It is possible that these values were a better start for the array feed and thereby found a better local optimum for it. If both feeds were designed using their optimum parameters maybe their relative performance would be different. To solve this problem, the optimization was tried using the global optimizer Basin-hoping [18] [19] as well. However, it ran for four days without starting to converge, so it was deemed to take to long to be feasible for this study.

Because of time limitations, the concept was only tested for a design which is not practically realizable, for several reasons. Firstly, the return loss was ignored in the optimization, which means that the gain of the antenna will be low. The sidelobe levels were also ignored, so it would not pass the regulations for satellite communication. Also, to be able to build the antenna, supports for the sub reflector would need to be added. Since the design is not realizable it is hard to draw any conclusions about any real antennas that could be built. However, the feed designed

in study did show some promise, and research in to a design which could be produced should be made.

5.2 Future Research and Possible Improvements

Some things could be tried to improve the optimization script. The feed antenna needs to be placed with its phase center at a specific spot. When D_h and L_h changes, the phase center moves. There is a parameter H_o which was meant to compensate for this. However, all of the parameters were independent, so the optimizer would have to find the optimum H_o every time it changed L_h or D_h. Because of this, the optimizer could have a hard time finding the optimum, making it take longer. To solve this, the phase reference point could be moved when D_h and L_h are changed. However, to do this, information about how the phase center moves depending on the parameters would be needed. During this study, no such formula was found.

Instead of using a local optimizer, a global optimization algorithm could be used. Like stated before, this was considered to be too slow for this study. There may be ways to speed it up though. Better settings could be used for the optimizer, and there may be another optimizer which is faster than Basin-hoping for this problem. A faster computer or a longer time frame would also solve this problem.

In the future, the concept of using a asymmetrical array to illuminate a truncated reflector should be tested on feeds which are practically realizable. The optimization should not only maximize the aperture efficiency, it should also minimize the return loss. It would also be interesting to see the concept tried for different feed types. For example, a hat feed [20] [21] [22] can be made to have low side lobes, low return loss and a wide bandwidth. Optimizing a hat feed to work with two waveguides could be a realizable solution. It would also be interesting to compare the two element array feed in this study to a single element feed with a contoured sub reflector, curved to create an elliptical radiation pattern [23].

5.3 Writing Optimization Script

Time became a limiting factor in this study. The reason for this is that more time had to be spent on setting up the optimizer than what was expected from the beginning. It was thought that CST could optimize towards arbitrary goals, which meant that nothing would have to be set up in Python. Figuring out how to control CST using Python, and then how to use this with an optimizer was no trivial task. In fact, most of the time spent in this study was on setting up the optimization script.

5.4 Societal and Ethical Aspects

Information and communication can be used for both good and bad. The antenna designed in this study is made for internet communication over satellites. Because the communication is over satellite, it enables people in areas where a ground based internet connection is not available to get access to the internet. This could give people in remote locations or in less developed countries access to the internet. Having an internet connection can open up many job opportunities and be a tool to improve someone's general life quality [24]. In some areas, the communication system on the ground can get shut down or destroyed, for example because of a conflict or a natural disaster. In these cases, an internet connection could aid a help organization in the area [25]. It is also a great asset for any journalist, who are important for spreading information about what is going on to the world. An internet connection would however also be helpful for any military organization. Depending on which side of the conflict you are on, this could either be detrimental or a saving grace.

6 Conclusion

Optimizing a two element array feed for the truncated main reflector in this study gave a higher simulated aperture efficiency than for a single element feed optimized with the same initial values. It is a possibility that an antenna utilizing a two element array feed could be built with a higher aperture efficiency than one utilizing a single element feed. However, more research has to be done before any real conclusion can be made since the feeds in this study were not practically realizable.

References

[1] "Types of orbits." (2020), [Online]. Available: https://www.esa.int/Enabling_Support/Space_Transportation/Types_of_orbits (visited on 01/18/2024).

[2] P.-S. Kildal, *Foundations of Antennas: A Unified Approach*. Lund: Studentlitteratur AB, 2000, ch. 1, 2, 8, 9, 10, ISBN: 91-44-01318-3.

[3] S. J. Orfanidis, *Electromagnetic Waves and Antennas*. 2016, ch. 2. [Online]. Available: http://eceweb1.rutgers.edu/~orfanidi/ewa/.

[4] A. Yaghjian, "An overview of near-field antenna measurements," *IEEE Transactions on Antennas and Propagation*, vol. 34, no. 1, pp. 30–45, 1986. DOI: 10.1109/TAP.1986.1143727.

[5] C. Shannon, "Communication in the presence of noise," *Proceedings of the IRE*, vol. 37, no. 1, pp. 10–21, 1949. DOI: 10.1109/JRPROC.1949.232969.

[6] C. Granet, "Designing axially symmetric cassegrain or gregorian dual-reflector antennas from combinations of prescribed geometric parameters," *IEEE Antennas and Propagation Magazine*, vol. 40, no. 2, pp. 76–82, 1998. DOI: 10.1109/74.683545.

[7] J. Zhang, P. Jiang, H. Yang, *et al.*, "Freeform reflector antenna design method to improve transmission efficiency and control output intensity distribution," *Appl. Opt.*, vol. 59, no. 25, pp. 7567–7573, Sep. 2020. DOI: 10.1364/AO.396623. [Online]. Available: https://opg.optica.org/ao/abstract.cfm?URI=ao-59-25-7567.

[8] P.-S. Kildal, "Factorization of the feed efficiency of paraboloids and cassegrain antennas," *IEEE Transactions on Antennas and Propagation*, vol. 33, no. 8, pp. 903–908, 1985. DOI: 10.1109/TAP.1985.1143689.

[9] SIMULIA. "Cst studio suite: Electromagnetic field simulation software," [Online]. Available: https://www.3ds.com/products/simulia/cst-studio-suite (visited on 05/21/2024).

[10] SIMULIA. "Cst python libraries," [Online]. Available: https://space.mit.edu/RADIO/CST_online/Python/main.html (visited on 05/20/2024).

[11] SIMULIA. "Vba objects overview," [Online]. Available: https://space.mit.edu/RADIO/CST_online/mergedProjects/VBA_3D/special_vbaobjects/special_vbaobjects_vbaobjects.htm (visited on 05/20/2024).

[12] J. A. Nelder and R. Mead, "A Simplex Method for Function Minimization," *The Computer Journal*, vol. 7, no. 4, pp. 308–313, Jan. 1965, ISSN: 0010-4620. DOI: 10.1093/comjnl/7.4.308. eprint: https://academic.oup.com/comjnl/article-pdf/7/4/308/1013182/7-4-308.pdf. [Online]. Available: https://doi.org/10.1093/comjnl/7.4.308.

[13] SciPy. "Minimize(method='nelder-mead')," [Online]. Available: https://docs.scipy.org/doc/scipy/reference/optimize.minimize-neldermead.html#optimize-minimize-neldermead (visited on 05/20/2024).

[14] "Numpy.trapz," [Online]. Available: https://numpy.org/doc/stable/reference/generated/numpy.trapz.html (visited on 05/25/2024).

[15] "Circular waveguide sizes table," [Online]. Available: http://www.qualwave.com/resources/circular-waveguide-sizes.htm (visited on 05/20/2024).

[16] "Electromagnetic simulation solvers: Cst studio suite simulation solvers for electromagnetic systems and devices," [Online]. Available: https://www.3ds.com/products/simulia/cst-studio-suite/electromagnetic-simulation-solvers (visited on 05/26/2024).

[17] V. Henkow. "Cst_optimization," [Online]. Available: https://github.com/victorhenkow/cst_optimization.git (visited on 06/04/2024).

[18] D. J. Wales and J. P. K. Doye, "Global optimization by basin-hopping and the lowest energy structures of lennard-jones clusters containing up to 110 atoms," *The Journal of Physical Chemistry A*, vol. 101, no. 28, pp. 5111–5116, 1997. DOI: 10.1021/jp970984n.

[19] "Scipy.optimize.basinhopping," [Online]. Available: https://docs.scipy.org/doc/scipy/reference/generated/scipy.optimize.basinhopping.html (visited on 05/28/2024).

[20] P.-S. Kildal, "The hat feed: A dual-mode rear-radiating waveguide antenna having low cross polarization," *IEEE Transactions on Antennas and Propagation*, vol. 35, no. 9, pp. 1010–1016, 1987. DOI: 10.1109/TAP.1987.1144221.

[21] J. Hansen, A. Kishk, P.-S. Kildal, and O. Dahlsjo, "High performance reflector hat antenna with very low sidelobes for radio-link applications," *IEEE Antennas and Propagation Society International Symposium. 1995 Digest*, vol. 2, 893–896 vol.2, 1995. [Online]. Available: https://api.semanticscholar.org/CorpusID:110620731.

[22] E. G. Geterud, J. Yang, T. Ostling, and P. Bergmark, "Design and optimization of a compact wideband hat-fed reflector antenna for satellite communications," *IEEE Transactions on Antennas and Propagation*, vol. 61, no. 1, pp. 125–133, 2013. DOI: 10.1109/TAP.2012.2220113.

[23] X. Liu, B. Du, J. Zhou, and L. Xie, "A low profile reflector antenna with large axial ratio elliptical beam," in *2022 International Conference on Microwave and Millimeter Wave Technology (ICMMT)*, 2022, pp. 1–3. DOI: 10.1109/ICMMT55580.2022.10022667.

[24] Y. Shaengchart and T. Kraiwanit, "Starlink satellite project impact on the internet provider service in emerging economies," *Research in Globalization*, vol. 6, p. 100 132, 2023, ISSN: 2590-051X. DOI: https://doi.org/10.1016/j.resglo.2023.100132. [Online]. Available: https://www.sciencedirect.com/science/article/pii/S2590051X23000229.

[25] H. Åkesson. "Göteborgsbaserade satellitbolaget tar nytt kliv – gör storaffär med global branschjätte." (Aug. 2023), [Online]. Available: https://www.breakit.se/artikel/37282/goteborgsbaserade-satellitbolaget-tar-nytt-kliv-gor-storaffar-med-global-branschjatte (visited on 06/01/2024).

Appendices

A LEO and GEO orbits

Satellites in geostationary orbits (GEO) circle earth from west to east [1] with an inclination with respect to the equator of $i = 0°$. They are placed at an altitude of 35786 km which makes them complete one orbital revolution in the same time it takes for the earth to spin around its own axis [1]. For an observer on earth this makes the satellite appear stationary in the sky. The benefit of this is that an antenna on earth can be fixed in place, always pointing towards the same spot in the sky. One disadvantage of GEO is that the satellite has to be at a high altitude which means that the distance the signal has to travel is long. This creates problems with for example low received power and with high latency. Satellites in low earth orbits (LEO) normally have an altitude < 1000 km but can be as low as 160 km [1], and their orbital plane can have any inclination with respect to the equator.

B Parabolic Reflector in Spherical Coordinates

A parabola can defined as the set of points where the distance from a point $|P|$ in the set to a fixed focus point F is equal to the distance from the point $|P|$ to a fixed line L orthogonal to the parabolas symmetry axis, called the directrix. With mathematical notation the set can be written as $\{P : |PF| = |PL|\}$. The point where the parabola intersects with the symmetry axis is called the vertex V. To be able to solve $|PF| = |PL|$ at the vertex of the parabola, the distance from the focus to the vertex must be equal to the distance from the directrix to the vertex, i.e $|FV| = |VL|$.

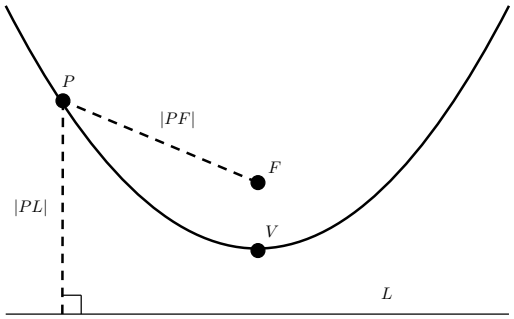

Figure 15: A parabola with its important features marked. L is the directrix, V is the vertex, F is the focal point and P is a general point on the parabola. $|PF|$ and $|PL|$ are indicated by the dashed lines.

The equation for a parabola with its focal point in the origin can be given by the following calculations. Assume a general point on the parabola $P = (x, y)$. The focus is at $F = (0, 0)$. $|FV| = |VL| = f \implies L = -2f$. This gives

$$|PF|^2 = |PL|^2 \iff (2f + y)^2 = x^2 + y^2 \iff y = \frac{x^2 - 4f^2}{4f} - f = \frac{x^2}{4f} - f. \tag{39}$$

The shape of the parabola can equivalently be parameterized using the angle θ, where $0 < \theta < \theta_0$ and θ_0 is the subtended half angle of the parabola. Using the defined directions in Figure 16 $x = r\sin(\theta)$ and $y = -r\cos(\theta)$. Equation (39) now becomes

$$-r\cos(\theta) = \frac{r^2\sin^2(\theta)}{4f} - f \iff r^2 = \frac{-4fr\cos(\theta) + 4f^2}{\sin^2(\theta/2)} \implies r = \frac{f}{\cos^2(\theta/2)}. \tag{40}$$

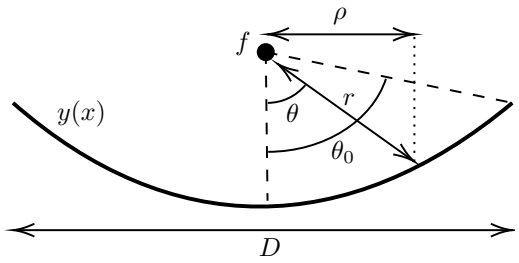

Figure 16: A parabola in terms of angles. θ_0 is the subtended half angle, ρ is radial point at the angle θ, r is the distance from the focal point f to the parabola and D is the diameter.

There are two solution to equation (40). However, one solution gives a parabola which is oriented the wrong way, so it can be ignored. The advantage of writing the equation in terms of θ is that it shows the required beamwidth of the feed antenna to illuminate the parabola. Using equation (40) the radius of the parabola can be expressed as

$$\rho = r\sin(\theta) = \frac{f\sin(\theta)}{\cos^2(\theta/2)} = \frac{2f\sin(\theta)}{1+\cos(\theta)} = 2f\tan(\theta/2). \tag{41}$$

The diameter of the reflector can now be expressed in terms of θ_0

$$D = 4f\tan(\theta_0/2). \tag{42}$$

C Circularly symmetric efficiency equations for parabolic reflector antennas

Equation for calculating the spillover efficiency, polarization efficiency, illumination efficiency and the phase efficiency of circularly symmetric antennas [8] are presented below.

$$e_{ill} = \frac{2}{\tan^2(\theta_0/2)} \frac{\left(\int_0^{\theta_0} |G_{co_{45^\circ}}(\theta)|\tan(\theta/2)d\theta\right)^2}{\int_0^{\theta_0} |G_{co_{45^\circ}}(\theta)|^2\sin(\theta)d\theta} \tag{43}$$

$$e_{\Phi} = \frac{\left|\int_0^{\theta_0} |G_{co_{45^\circ}}(\theta)|e^{j\Phi}\tan(\theta/2)d\theta\right|^2}{\left(\int_0^{\theta_0} |G_{co_{45^\circ}}(\theta)|\tan(\theta/2)d\theta\right)^2} \tag{44}$$

$$e_{pol} = \frac{\int_0^{\theta_0} |G_{co_{45^\circ}}(\theta)|^2\sin(\theta)d\theta}{\int_0^{\theta_0} (G_{co_{45^\circ}}(\theta)|^2 + |G_{xp_{45^\circ}}(\theta)|^2)\sin(\theta)d\theta} \tag{45}$$

$$e_{sp} = \frac{\int_0^{\theta_0} (|G_{co_{45^\circ}}(\theta)|^2 + |G_{xp_{45^\circ}}(\theta)|^2)\sin(\theta)d\theta}{\int_0^{\pi} (|G_{co_{45^\circ}}(\theta)|^2 + |G_{xp_{45^\circ}}(\theta)|^2)\sin(\theta)d\theta} \tag{46}$$

DEPARTMENT OF ELECTRICAL ENGINEERING
CHALMERS UNIVERSITY OF TECHNOLOGY
Gothenburg, Sweden 2024
www.chalmers.se

CHALMERS